

See discussions, stats, and author profiles for this publication at: <https://www.researchgate.net/publication/11407857>

# Formation and characterization of the gallium and indium subhydride molecules $\text{Ga}_2\text{H}_2$ and $\text{In}_2\text{H}_2$ : a matrix isolation study.

ARTICLE *in* JOURNAL OF THE AMERICAN CHEMICAL SOCIETY · APRIL 2002

Impact Factor: 12.11 · Source: PubMed

---

CITATIONS

12

---

READS

55

## 4 AUTHORS, INCLUDING:



**Anthony J Downs**

University of Oxford

258 PUBLICATIONS 5,070 CITATIONS

SEE PROFILE



**Pluton Pullumbi**

Air Liquide

45 PUBLICATIONS 626 CITATIONS

SEE PROFILE

## Formation and Characterization of the Gallium and Indium Subhydride Molecules $\text{Ga}_2\text{H}_2$ and $\text{In}_2\text{H}_2$ : A Matrix Isolation Study

Hans-Jörg Himmel,<sup>\*,†</sup> Laurent Manceron,<sup>‡</sup> Anthony J. Downs,<sup>§</sup> and Pluton Pullumbi<sup>||</sup>

Contribution from the Institut für Anorganische Chemie der Universität Karlsruhe, Engesserstrasse, Geb. 30.45, 76128 Karlsruhe, Germany, LADIR/Equipe de Spectrochimie Moléculaire, CNRS UMR, Université Pierre et Marie Curie, Case courrier 49, 4 Place Jussieu, 75252, Paris Cedex 05, France, Inorganic Chemistry Laboratory, University of Oxford, South Parks Road, Oxford OX1 3QR, United Kingdom, and Air Liquide, Centre de Recherche Claude-Delorme, 1, Chemin de la porte des Loges, BP 126, Les Loges-en Josas, France

Received October 2, 2001

**Abstract:**  $\text{Ga}_2$  reacts spontaneously with  $\text{H}_2$  in solid Ar matrixes at 12 K to form the cyclic molecule  $\text{Ga}(\mu\text{-H})_2\text{Ga}$ .  $\text{In}_2$  does not react with  $\text{H}_2$  under similar conditions, but irradiation at wavelengths near 365 nm induces the formation of the corresponding indium hydride,  $\text{In}(\mu\text{-H})_2\text{In}$ . The molecules have been identified and characterized by the IR spectra displayed by matrixes containing the metal and  $\text{H}_2$ ,  $\text{D}_2$ , HD, or  $\text{H}_2 + \text{D}_2$ ; they each have planar, dihydrido-bridged structures with  $D_{2h}$  symmetry, as endorsed by comparison of the measured spectra (i) with the properties forecast by quantum chemical calculations and (ii) with the spectra of known gallium and indium hydrides. Both are photolabile under visible light ( $\lambda > 450$  nm): green light ( $\lambda = \text{ca. } 546$  nm) causes  $\text{Ga}(\mu\text{-H})_2\text{Ga}$  to isomerize to a mixture of  $\text{HGaGaH}$  and  $\text{H}_2\text{GaGa}$ , whereas broad-band visible irradiation ( $\lambda > 450$  nm) of  $\text{In}(\mu\text{-H})_2\text{In}$  gives rise to the isomer  $\text{HInInH}$ , together with  $\text{InH}$ . The isomerization can be reversed by UV photolysis ( $\lambda = \text{ca. } 365$  nm) of  $\text{HGaGaH}$ ,  $\text{H}_2\text{GaGa}$ , and  $\text{HInInH}$  or by near-IR photolysis ( $\lambda > 700$  nm) of  $\text{HGaGaH}$  and  $\text{H}_2\text{GaGa}$ .

### Introduction

Since the first report of gallane,  $[\text{GaH}_3]_n$ , as an authenticated product in 1989,<sup>1</sup> a crop of other gallium hydrides has been synthesized and characterized.<sup>2</sup> The simplest, mononuclear species,  $\text{GaH}$ ,  $\text{GaH}_2$ , and  $\text{GaH}_3$ , can be generated only as transients in the gas phase<sup>3–6</sup> but may be preserved in solid noble gas matrixes following the reaction of Ga atoms with  $\text{H}_2$  molecules or H atoms.<sup>7–9</sup> Stabilization results (i) from aggregation, as in the dimeric  $\text{H}_2\text{Ga}(\mu\text{-H})_2\text{GaH}_2$ , which has been characterized in the gas phase at near-ambient temperatures;<sup>1</sup> (ii) from substitution of hydride by other ligands, as in  $[\text{H}_2\text{-}$

$\text{GaCl}]_n$ <sup>10</sup> and  $\text{HGa}(\text{BH}_4)_2$ ;<sup>11</sup> or (iii) from complexation,<sup>5,6,12</sup> as in  $\text{Me}_3\text{N}\cdot\text{GaH}_3$ <sup>13</sup> and  $\text{HC}(\text{CH}_2\text{CH}_2)_3\text{N}\cdot\text{GaH}_3$ .<sup>14</sup>

On the other hand, indium hydrides are still a rarity.<sup>5,6</sup> The mononuclear molecules  $\text{InH}_n$  ( $n = 1\text{--}3$ ) have all been characterized either in the gas phase ( $n = 1$ )<sup>5,6</sup> or in the matrix-isolated state,<sup>8,9</sup> but quantum chemical calculations offer little prospect of lasting stability to indane, even as an oligomer or polymer,  $[\text{InH}_3]_n$ .<sup>15</sup> Stabilization of  $\text{InH}_3$  may be achieved by complexation with a suitably strong and bulky base, e.g.,  $:\text{CN}(\text{Mes})\text{-C}_2\text{H}_4\text{N}(\text{Mes})$  ( $\text{Mes} = 1,3,5\text{-Me}_3\text{C}_6\text{H}_2$ ),<sup>16a</sup>  $:\text{CN}(\text{Pr}^i)\text{C}_2\text{Me}_2\text{N-}(\text{Pr}^i)$ ,<sup>16b</sup> and  $\text{PCy}_3$ .<sup>16c</sup> Otherwise greater stability can be achieved

\* To whom correspondence should be addressed.

† Institut für Anorganische Chemie der Universität Karlsruhe

‡ Université Pierre et Marie Curie.

§ University of Oxford.

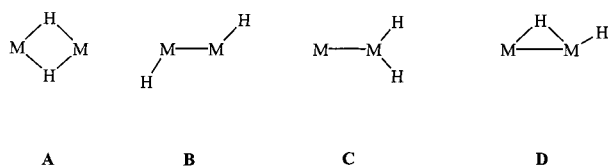
|| Centre de Recherche Claude-Delorme.

- (1) (a) Downs, A. J.; Goode, M. J.; Pulham, C. R. *J. Am. Chem. Soc.* **1989**, *111*, 1936–1937. (b) Pulham, C. R.; Downs, A. J.; Goode, M. J.; Rankin, D. W. H.; Robertson, H. E. *J. Am. Chem. Soc.* **1991**, *113*, 5149–5162.
- (2) Taylor, M. J.; Brothers, P. J. In *Chemistry of Aluminium, Gallium, Indium and Thallium*; Downs, A. J., Ed.; Blackie: Glasgow, U.K., 1993; pp 111–247.
- (3) Downs, A. J.; Pulham, C. R. *Adv. Inorg. Chem.* **1994**, *41*, 171–232.
- (4) Downs, A. J.; Pulham, C. R. *Chem. Soc. Rev.* **1994**, *23*, 175–184.
- (5) Downs, A. J. *Coord. Chem. Rev.* **1999**, *189*, 59–100.
- (6) Aldridge, S.; Downs, A. J. *Chem. Rev.* **2001**, *101*, 3305–3365.
- (7) Xiao, Z. L.; Hauge, R. H.; Margrave, J. L. *Inorg. Chem.* **1993**, *32*, 642–646.
- (8) Pullumbi, P.; Mijoule, C.; Manceron, L.; Bouteiller, Y. *Chem. Phys.* **1994**, *185*, 13–24.
- (9) Pullumbi, P.; Bouteiller, Y.; Manceron, L.; Mijoule, C. *Chem. Phys.* **1994**, *185*, 25–37.

- (10) (a) Johnsen, E.; Downs, A. J.; Greene, T. M.; Souter, P. F.; Aarset, K.; Page, E. M.; Rice, D. A.; Richardson, A. N.; Brain, P. T.; Rankin, D. W. H.; Pulham, C. R. *Inorg. Chem.* **2000**, *39*, 719–727. (b) Johnsen, E.; Downs, A. J.; Goode, M. J.; Greene, T. M.; Himmel, H.-J.; Müller, M.; Parsons, S.; Pulham, C. R. *Inorg. Chem.* **2001**, *40*, 4755–4761.
- (11) (a) Downs, A. J.; Greene, T. M.; Harman, L. A.; Souter, P. F.; Brain, P. T.; Pulham, C. R.; Rankin, D. W. H.; Robertson, H. E.; Hofmann, M.; Schleyer, P. v. R. *Inorg. Chem.* **1995**, *34*, 1799–1809. (b) Downs, A. J.; Harman, L. A.; Thomas, P. D. P.; Pulham, C. R. *Polyhedron* **1995**, *14*, 935–945.
- (12) Gardiner, M. G.; Raston, C. L. *Coord. Chem. Rev.* **1997**, *166*, 1–34.
- (13) Brain, P. T.; Brown, H. E.; Downs, A. J.; Greene, T. M.; Johnsen, E.; Parsons, S.; Rankin, D. W. H.; Smart, B. A.; Tang, C. Y. *J. Chem. Soc., Dalton Trans.* **1998**, 3685–3691.
- (14) Atwood, J. L.; Bott, S. G.; Elms, F. M.; Jones, C.; Raston, C. L. *Inorg. Chem.* **1991**, *30*, 3792–3793.
- (15) Hunt, P.; Schwerdtfeger, P. *Inorg. Chem.* **1996**, *35*, 2085–2088.
- (16) (a) Abernethy, C. D.; Cole, M. L.; Jones, C. *Organometallics* **2000**, *19*, 4852–4857. (b) Hibbs, D. E.; Hursthouse, M. B.; Jones, C.; Smithies, N. A. *J. Chem. Soc., Chem. Commun.* **1998**, 869–870. (c) Hibbs, D. E.; Jones, C.; Smithies, N. A. *J. Chem. Soc., Chem. Commun.* **1999**, 185–186.

only by substitution of one or more hydride ligands and/or Coulombic interactions, as in the anionic complexes  $M^+[R_3-InHInR_3]^-$  [where  $M = Li(Me_2NC_2H_4NMe_2)_2$  and  $R = Me^{17a}$  or  $M = K$  and  $R = CH_2CMe_3^{17b}$ ], which are notable for featuring In–H–In bridges.

Subhydrides of the group 13 elements (M) of the type  $[MH]_2$  have attracted theoretical attention despite a dearth of hard experimental fact. Diborene,  $B_2H_2$ , has a linear triplet ground state involving little or no B–B double bonding.<sup>18</sup> By contrast, a bis( $\mu$ -hydrido) structure A with  $D_{2h}$  symmetry is calculated to be the most stable form for all the other group 13 elements.<sup>4,6,19,20</sup> Instead of the linear form, which is now only a transition state, a *trans*-bent isomer B ( $C_{2h}$ ) appears as a second minimum on the PE surface, and there are two other possible isomers, namely, the asymmetric M–MH<sub>2</sub>, structure C ( $C_{2v}$ ), and mono-H-bridged HM( $\mu$ -H)M, structure D ( $C_s$ ), giving minima at energies not far above the global minimum. The IR spectra of Ar matrixes formed by condensing laser-ablated Al atoms with H<sub>2</sub> include absorptions attributable to isomers A and possibly D for M = Al.<sup>21</sup> Similar experiments with thermally evaporated gallium have suggested<sup>7</sup> that the dimer Ga<sub>2</sub> reacts spontaneously with H<sub>2</sub> to form isomer A for M = Ga.



Here we describe the results of detailed experiments aimed at investigating the thermally and/or photolytically activated reactions that occur in Ar matrixes containing M<sub>2</sub> dimers (M = Ga or In) and H<sub>2</sub>. The course of events has been tracked through the IR spectra of the matrixes, and the identities of the products have been confirmed (i) by carrying out experiments with D<sub>2</sub>, HD, or an H<sub>2</sub>/D<sub>2</sub> mixture in place of H<sub>2</sub>; (ii) by comparison with the results of quantum chemical calculations at different levels of theory; and (iii) by reference to the properties of related molecules. Hence we will show that H<sub>2</sub> adds to Ga<sub>2</sub> spontaneously, and to In<sub>2</sub> only on photolysis at  $\lambda = ca. 365$  nm, to form the dihydrido-bridged molecules Ga( $\mu$ -H)<sub>2</sub>Ga, **1a**, and In( $\mu$ -H)<sub>2</sub>In, **1b**, respectively. Neither of these products is photostable. Irradiation with visible light ( $\lambda > 450$  nm) causes isomerization to the *trans*-bent species HGaGaH, **2a**, and HInInH, **2b**, in a process that can be reversed by UV photolysis ( $\lambda = ca. 365$  nm). In the case of Ga( $\mu$ -H)<sub>2</sub>Ga irradiation with green light ( $\lambda = ca. 546$  nm) gives access not only to the second isomer **2a** but also to a third believed to be H<sub>2</sub>GaGa, **3a**.

## Experimental Section

Gallium (Aldrich, purity 99.9999%) and indium (Aldrich, purity 99.9999%) were each evaporated from either a tantalum or a graphite cell or a tungsten filament that was heated resistively to ca. 900 °C. Hence the metal vapor was co-deposited with an excess of H<sub>2</sub>-doped argon on a CsI window or the face of a highly polished copper block cooled to 10–12 K by means of a closed-cycle refrigerator (Air Products CS 202 or Leybold LB 510).<sup>8,9,22–24</sup> The proportions M:H<sub>2</sub>:Ar (M = Ga or In) were typically 0.5:0.5:100 and 0.5:1:100, as estimated with a microbalance, while deposition rates were ca. 2 mmol of matrix gas h<sup>–1</sup>, continued over a period of 1.5 h. Similar experiments were carried out with D<sub>2</sub>, HD, or a 1:1 H<sub>2</sub>/D<sub>2</sub> mixture in place of H<sub>2</sub>.

The following materials were used as received from the sources and with the stated purities listed: H<sub>2</sub> (Air Liquide, 99.995%), D<sub>2</sub> (Isotec, 99.5%), HD (prepared by reaction of LiAlH<sub>4</sub> with D<sub>2</sub>O and passed through a liquid N<sub>2</sub> trap, ca. 90% HD and 10% H<sub>2</sub>), and argon (Messer, purity 4.8). Gas mixtures of argon with the different isotopic versions of dihydrogen were prepared by standard manometric methods.

Photolysis was brought about with a high-pressure Xe/Hg arc or a medium-pressure Hg lamp (Philips LP 125) operating at 200 or 125 W, respectively, IR radiation being absorbed by a water filter so as to minimize any heating effects. Light of the desired wavelengths was delivered via appropriate interference or Pyrex filters.

IR spectra of the matrix samples were recorded mostly in reflection at resolutions ranging from 0.5 to 0.05 cm<sup>–1</sup> and with a wavenumber accuracy of  $\pm 0.1$  cm<sup>–1</sup>. Three different FTIR spectrometers were used, viz., a Nicolet Magna-IR 560 (at Oxford), a Bruker 113v (at Karlsruhe), and a Bruker 120 (at Paris).

Quantum chemical calculations were performed with the aid of the GAUSSIAN 98 program package.<sup>25</sup> Use was made of ab initio (MP2) as well as pure DFT (B3PW91) and the B3LYP hybrid method, which has been shown to give satisfactory results for small aluminum and gallium compounds.<sup>26</sup> A 6-311G(d) basis set was used for Ga, and a LANL2DZ one with additional d-polarization functions (exponent 0.5) for In.

## Results

The vapors over gallium and indium metals at ca. 900 °C are known to contain not only atoms but also a small but significant fraction of the dimers Ga<sub>2</sub> and In<sub>2</sub>, respectively. Previous spectroscopic studies have shown these dimers to be trapped in the matrixes formed by co-condensing the metal vapors with an excess of a noble gas.<sup>7,27,28</sup> The photoinduced reactions of the atoms with H<sub>2</sub> and H atoms under these conditions have already been described.<sup>7–9</sup> Here we are concerned exclusively with the dimers and their reaction with

- (17) (a) Hibbs, D. E.; Hursthouse, M. B.; Jones, C.; Smithies, N. A. *Organometallics* **1998**, *17*, 3108–3110. (b) Beachley, O. T., Jr.; Chao, S.-H. L.; Churchill, M. R.; See, R. F. *Organometallics* **1992**, *11*, 1486–1491.
- (18) (a) Knight, L. B., Jr.; Kerr, K.; Miller, P. K.; Arrington, C. A. *J. Phys. Chem.* **1995**, *99*, 16842–16848. (b) Tague, T. J., Jr.; Andrews, L. *J. Am. Chem. Soc.* **1994**, *116*, 4970–4976.
- (19) (a) Palágyi, Z.; Grev, R. S.; Schaefer, H. F., III *J. Am. Chem. Soc.* **1993**, *115*, 1936–1943. (b) Palágyi, Z.; Schaefer, H. F., III *Chem. Phys. Lett.* **1993**, *203*, 195–200. (c) Yamaguchi, Y.; DeLeeuw, B. J.; Richards, C. A., Jr.; Schaefer, H. F., III; Frenking, G. *J. Am. Chem. Soc.* **1994**, *116*, 11922–11930.
- (20) Treboux, G.; Barthelat, J.-C. *J. Am. Chem. Soc.* **1993**, *115*, 5, 4870–4878.
- (21) Stephens, J. C.; Bolton, E. E.; Schaefer, H. F., III; Andrews, L. *J. Chem. Phys.* **1997**, *107*, 119–123.

- (22) Himmel, H.-J.; Downs, A. J.; Greene, T. M.; Andrews, L. *Organometallics* **2000**, *19*, 1060–1070.
- (23) See, for example: Zumbusch, A.; Schnöckel, H. *J. Chem. Phys.* **1998**, *108*, 8092–8100.
- (24) Manceron, L.; Loutellier, A.; Perchard, J. P. *Chem. Phys.* **1985**, *92*, 75–89.
- (25) Frisch, M. J.; Trucks, G. W.; Schlegel, H. B.; Scuseria, G. E.; Robb, M. A.; Cheeseman, J. R.; Zakrzewski, V. G.; Montgomery, J. A., Jr.; Stratmann, R. E.; Burant, J. C.; Dapprich, S.; Millam, J. M.; Daniels, A. D.; Kudin, K. N.; Strain, M. C.; Farkas, O.; Tomasi, J.; Barone, V.; Cossi, M.; Cammi, R.; Mennucci, B.; Pomelli, C.; Adamo, C.; Clifford, S.; Ochterski, J.; Petersson, G. A.; Ayala, P. Y.; Cui, Q.; Morokuma, K.; Malick, D. K.; Rabuck, A. D.; Raghavachari, K.; Foresman, J. B.; Cioslowski, J.; Ortiz, J. V.; Stefanov, B. B.; Liu, G.; Liashenko, A.; Piskorz, P.; Komaromi, I.; Gomperts, R.; Martin, R. L.; Fox, D. J.; Keith, T.; Al-Laham, M. A.; Peng, C. Y.; Nanayakkara, A.; Gonzalez, C.; Challacombe, M.; Gill, P. M. W.; Johnson, B. G.; Chen, W.; Wong, M. W.; Andres, J. L.; Head-Gordon, M.; Replogle, E. S.; Pople, J. A. *Gaussian 98*, revision A.3; Gaussian, Inc.: Pittsburgh, PA, 1998.
- (26) Jursic, B. S. *J. Mol. Struct.: THEOCHEM* **1998**, *428*, 61–66.
- (27) Douglas, M. A.; Hauge, R. H.; Margrave, J. L. *J. Phys. Chem.* **1983**, *87*, 2945–2947.
- (28) Froben, F. W.; Schulze, W.; Kloss, U. *Chem. Phys. Lett.* **1983**, *99*, 500–502. Balasubramanian, K.; Li, J. *J. Chem. Phys.* **1988**, *88*, 4979–4986.

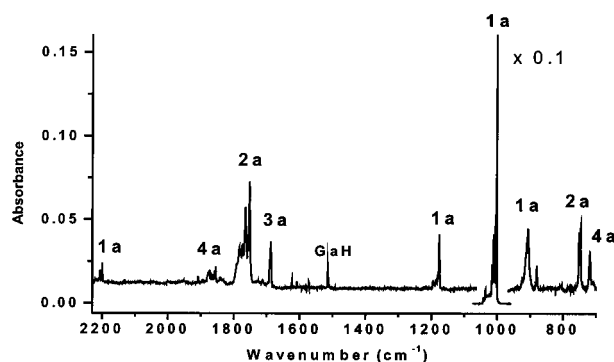


**Figure 1.** Infrared spectra in the region 2300–700  $\text{cm}^{-1}$  for an Ar matrix containing Ga vapor co-deposited with  $\text{H}_2$ :  $\text{Ga}/\text{H}_2/\text{Ar} = 0.6/1/100$  deposited at 14 K for 90 min. The absorbance scale in the 1100–950  $\text{cm}^{-1}$  region is divided by 10 for ease of presentation.

$\text{H}_2$ , and with the photochemistries of the products. The results will be reported in turn for gallium and indium. Spectroscopic features have been assigned on the basis of the following criteria: (i) their growth and decay characteristics in response to photolysis of the matrix for different times and under different conditions, e.g., of reagent concentration; (ii) comparisons with the results of control experiments that did not include one of the reagents or with the spectra of related species; (iii) consideration of the selection rules expected to govern the IR activity of a given molecule; (iv) the observed effects of the naturally occurring  $^{69}\text{Ga}$  and  $^{71}\text{Ga}$  isotopes and of deuteration of the dihydrogen precursor; and (v) appraisal of the measured spectroscopic properties in the light of those forecast by DFT calculations.

**Digallium,  $\text{Ga}_2$ .** As demonstrated first by Xiao et al.,<sup>7</sup> co-condensation of gallium vapor with an excess of argon doped with different amounts of dihydrogen (with  $\text{H}_2/\text{Ar}$  molar ratios varying from 1:1000 to 150:1000) gave matrixes that displayed new IR absorption bands. These features are quite distinct from the weak bands associated with the products formed by the reaction of gallium atoms with hydrogen,<sup>8,9</sup> water,<sup>29</sup> carbon monoxide,<sup>30</sup> or carbon dioxide,<sup>31</sup> the last three being present as trace impurities (see Figure 1). The most intense of the new bands appeared at 1002  $\text{cm}^{-1}$  with others weaker by an order of magnitude or more located at 2200, 1875, 1855, 1750, 1686, 1176, 951, 906.5, 880, 752/747, and 718  $\text{cm}^{-1}$ . A very characteristic growth pattern became evident when the proportion of gallium in the matrix was increased. Typically, it was observed that the strongest band experienced 4–40-fold increases of intensity when the  $\text{Ga}:\text{Ar}$  molar ratio was raised from 1:1000 to 2:1000 and next to 6:1000. Such a quadratic dependence on the metal concentration gives clear notice that the new species contains *two* metal atoms.

Systematic studies of the effects of hydrogen concentration and of selective photoexcitation make it possible to group all the new absorptions in four sets associated with four distinct molecules labeled **1a**, **2a**, **3a**, and **4a** in Table 1. The last family due to **4a** consists of weak absorptions near 1875, 1855, and 718  $\text{cm}^{-1}$  that exhibited marked growth with respect to the other families when the hydrogen concentration was increased. **4a**

**Table 1.** Wavenumbers of IR Bands Observed for Ar Matrixes Containing  $\text{Ga}_2$  and  $\text{H}_2/\text{D}_2/\text{HD}$ <sup>a</sup>

$\text{H}_2$	$\text{D}_2$	$\text{HD}$	deposition	photolysis			absorber
				$\lambda = 546 \text{ nm}$	$\lambda = 400 \text{ nm}$	$\lambda = 365 \text{ nm}$ or $>700 \text{ nm}$	
2200	1592	2040	↑	↓		↑	<b>1a</b>
1875				↑			<b>4a</b>
1855				↑			<b>4a</b>
1765.1	1275.8	1758.0		↑	↑	↓	<b>2a</b>
1752.1	1260.1	1269.6		↑	↑	↓	<b>2a</b>
1686.1	1206.4			↑	↓	↓	<b>3a</b>
1177.4	907.2	$\approx 1128$					
1176.1	905.9		↑	↓		↑	<b>1a</b>
1174.8	904.8						
1002	728	953	↑	↓		↑	<b>1a</b>
951	951	951	↑				<b>5a</b>
906.5	653.6	849	↑	↓		↑	<b>1a</b>
880	638.4	675.7	↑	↓		↑	<b>1a</b>
752.1	540.3	660.6					
747.0	536.9	655.4		↑	↑	↓	<b>2a</b>
718				↑			<b>4a</b>

<sup>a</sup> Wavenumbers are given in reciprocal centimeters.

must therefore contain more hydrogen than the other species **1a**, **2a**, and **3a**, the absorptions of which maintained a more or less linear dependence of intensity on the dihydrogen concentration. While the bands belonging to these three products are all characterized by the same second- and first-order dependences on the Ga and  $\text{H}_2$  concentrations, respectively, they can be differentiated easily by the very specific photosensitivity of the products to near-IR, visible, or UV light. Species **5a** with only one weak absorption at 951  $\text{cm}^{-1}$  showed no shift upon isotopic substitution and is likely therefore to arise from a reaction between  $\text{Ga}_2$  and traces of  $\text{H}_2\text{O}$  in the matrix.

The most prominent absorptions observed immediately after deposition of the matrixes were those at 2200, 1176, 1002, 906.5, and 880  $\text{cm}^{-1}$  attributable to species **1a**. On the other hand, exposure of the matrix to 546 nm light caused the efficient conversion of this molecule to **2a** and **3a**. Blue light with wavelengths of 400–440 nm was observed to induce a slow and limited reversion to **1a**, a change accomplished completely with either near-UV light ( $\lambda = \text{ca. } 365 \text{ nm}$ ) or near-IR light ( $\lambda > 700 \text{ nm}$ ) (Figure 2).

**Species 1a** is distinguished by a very strong IR absorption centered near 1002  $\text{cm}^{-1}$ , which displayed a large shift (to 728  $\text{cm}^{-1}$ ) when  $\text{H}_2$  was replaced by  $\text{D}_2$  but a much smaller one (to 953  $\text{cm}^{-1}$ ) when  $\text{H}_2$  was replaced by HD. These absorptions had been reported previously by Xiao et al.,<sup>7</sup> who linked them, as we do, to the dihydrido-bridged species  $\text{Ga}(\mu\text{-H})_2\text{Ga}$ . The present study has brought to light several more signals attributable to the same molecule, namely, a relatively strong absorption near 906.5  $\text{cm}^{-1}$  and three much weaker ones near 2200, 1176, and 880  $\text{cm}^{-1}$  (Figures 1 and 2). As illustrated in Figure 2, each of the bands presented either a complex and asymmetric profile (as at 906.5  $\text{cm}^{-1}$ ) or a multiplicity of closely spaced satellites adjacent to the main feature. The intensity distribution between the neighboring signals did not change even when the reagent concentrations were varied widely but did alter in response to different sample treatments (namely, annealing or back-conversion after the various photolytic cycles). It follows that the signal multiplicity observed for each transition can be related to inhomogeneous broadening and extensive trapping site effects for a highly deformable molecule. Systematic studies located the multiplet component pertaining in each case to the *main*

(29) Hauge, R. H.; Kauffman, J. W.; Margrave, J. L. *J. Am. Chem. Soc.* **1980**, *102*, 6005–6011.

(30) Himmel, H.-J.; Downs, A. J.; Green, J. C.; Greene, T. M. *J. Phys. Chem. A* **2000**, *104*, 3642–3654.

(31) Xu, C.; Manceron, L.; Perchard, J. P. *J. Mol. Struct.* **1993**, *300*, 83–92.



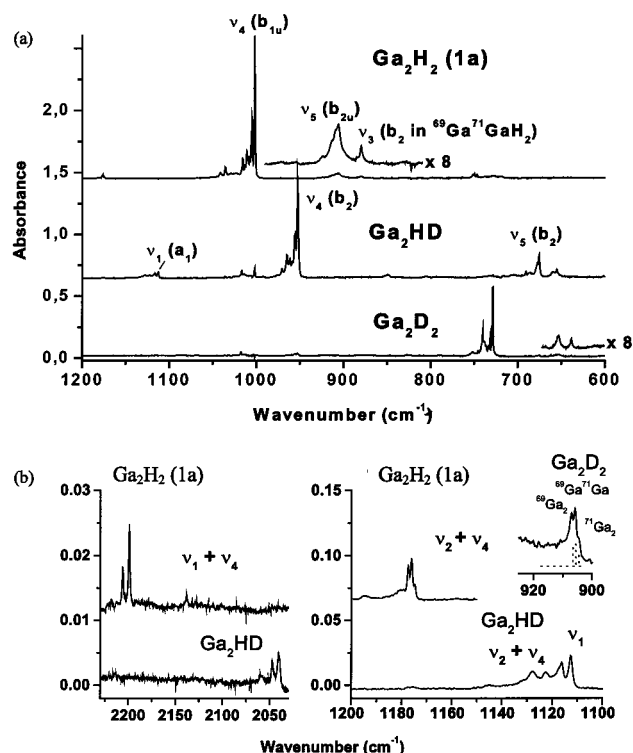


**Figure 2.** (a) Infrared spectra in the region 1200–600 cm<sup>-1</sup> for an Ar matrix containing Ga vapor co-deposited with 1% of different dihydrogen isotopomers: (upper spectrum) H<sub>2</sub>, (middle spectrum) HD, and (lower spectrum) D<sub>2</sub>. (b) Infrared spectra in the region 2250–2040 cm<sup>-1</sup> for Ga + H<sub>2</sub>, Ga + HD, and Ga + D<sub>2</sub> in an Ar matrix: Ga/H<sub>2</sub>/Ar = Ga/HD/Ar = Ga/D<sub>2</sub>/Ar = 0.3/1/100.

trapping site. For the sake of simplicity, the rest of the discussion will refer only to these wavenumbers (as in Table 1).

Experiments were performed with mixtures of H<sub>2</sub> and D<sub>2</sub> but under no circumstances did the samples reveal absorptions different from those observed in experiments involving H<sub>2</sub> and D<sub>2</sub> severally. There was in particular no trace of an absorption implying the formation of a mixed hydride–deuteride species. Hence concerted addition of H<sub>2</sub> to Ga<sub>2</sub> appears to be confirmed. With due allowance for the possible effects of matrix splitting, it is noteworthy too that the weak absorption at 1176 cm<sup>-1</sup> associated with the H<sub>2</sub> product displayed a *triplet* pattern with closely spaced components at 1177.4, 1176.1, and 1174.8 cm<sup>-1</sup> (see Figure 2b). The relative intensities of the components approximate the ratios 2.3:3.0:1 expected for a statistical mixture of the naturally occurring isotopes <sup>69</sup>Ga (60.1%) and <sup>71</sup>Ga (39.9%) distributed over *two equivalent* sites in **1a**. A similar pattern can be discerned in the band centered near 907 cm<sup>-1</sup> in the spectrum of the D<sub>2</sub> product.

Comparison of the outcome of experiments with D<sub>2</sub> with that of experiments involving either H<sub>2</sub> or HD discloses a striking difference in the product yield achieved immediately after sample deposition. Depending on the experimental conditions, the bands due to the perdeuterated version of **1a** initially reached only 30–40% of their expected intensities. However, the bands were observed to grow slowly over a period of several hours with the unirradiated sample kept at 10–12 K, to reach ultimately the intensity levels consistent with the normal product yield. This process was accelerated if the sample was exposed to additional IR radiation (coming from either the spectrometer source or a more luminous external IR source). Experiments

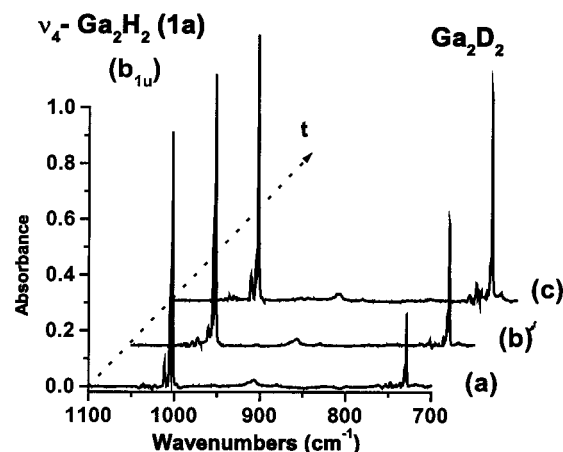


**Figure 3.** Infrared spectra in the region 1100–700 cm<sup>-1</sup> for gallium vapor co-deposited with H<sub>2</sub>/D<sub>2</sub>/Ar = 0.4/0.6/100 for 120 min at 14 K: (a) immediately after deposition; (b) after 12 h; and (c) after 20 h and exposure to IR light.

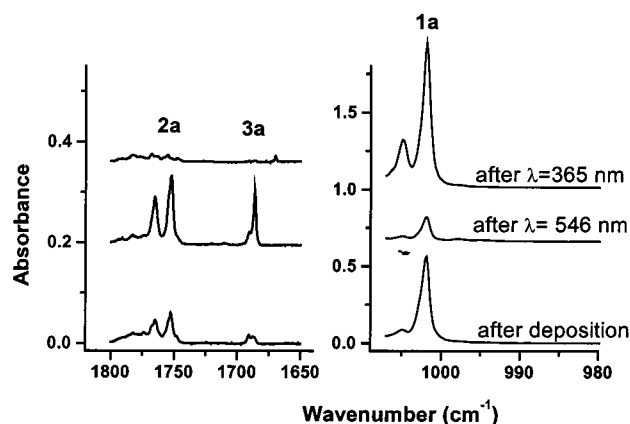


**Figure 4.** Infrared spectra in the regions 1800–1650 and 1020–990 cm<sup>-1</sup> for an Ar matrix containing Ga vapor co-deposited with H<sub>2</sub> showing the effects of photolysis.

run with band-pass interference filters identified the wavenumber range for efficient conversion as lying between 4500 and 3200 cm<sup>-1</sup>, a domain where no significant absorption could be detected. This kinetic isotope effect is best exemplified in two separate experiments carried out with matrixes containing comparable amounts of H<sub>2</sub> and D<sub>2</sub> and submitted to the same experimental conditions, with the results illustrated in Figure 3.

**Species 2a.** Although this product was present in low concentrations directly after deposition, its formation was observed to be fostered by photochemical processes at the expense of **1a** (see Figures 1 and 4). Its strongest IR absorptions correspond to features reported previously by Xiao et al.<sup>7</sup> and tentatively assigned by them to a Ga<sub>3</sub>H<sub>2</sub> molecule. It is characterized by a pair of absorptions of roughly equal intensity at 1765.1 and 1752.1 cm<sup>-1</sup> and a single absorption near 752 cm<sup>-1</sup>. The first two thus occur in the region associated with the stretching fundamentals of terminal Ga–H bonds where the gallium is in a low formal oxidation state, and the wavenumber of the third falls in the region characteristic of H–Ga–H bending modes.<sup>7–9,22,32,33</sup> Indeed, the wavenumbers of all three bands are not far from those of the three fundamentals of the GaH<sub>2</sub> triatomic.<sup>8</sup> Replacement of H<sub>2</sub> by D<sub>2</sub> was observed to result in shifts to 1275.8, 1260.1, and 540.3 cm<sup>-1</sup>, corresponding

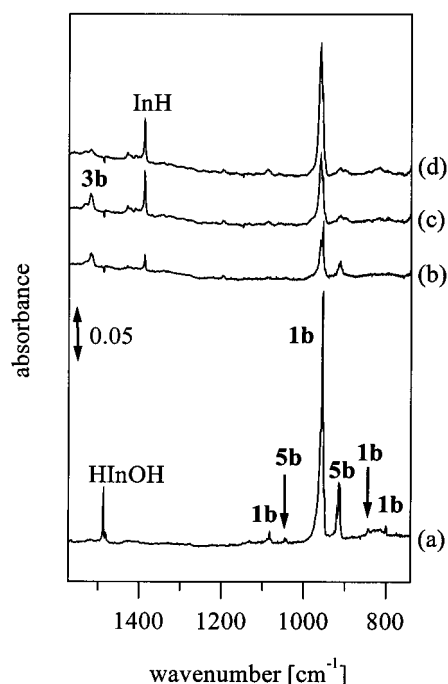


**Figure 5.** Infrared spectra recorded for an Ar matrix containing In vapor and 5% H<sub>2</sub>: (a) following photolysis at  $\lambda = 365$  nm; (b) after photolysis with light having  $\lambda > 450$  nm; (c) after broad-band UV–visible photolysis ( $200 \leq \lambda \leq 800$  nm); and (d) after a second cycle of photolysis at  $\lambda = 365$  nm.

to H/D = 1.3835:1, 1.3904:1, and 1.3918:1, respectively. By contrast, experiments with HD gave bands with intermediate wavenumbers, viz., 1758, 1269.6, and 655.4 cm<sup>−1</sup>.

**Species 3a.** This is a very minor product after deposition. Again, however, it is produced at the expense of **1a** on excitation with green light ( $\lambda =$  ca. 546 nm), but is converted to **2a** either by annealing of the matrix at temperatures up to 25–30 K or by irradiation with near-UV light ( $\lambda =$  ca. 365 nm). All the evidence available suggests therefore that **3a** is a third tautomeric form of Ga<sub>2</sub>H<sub>2</sub>. It was observed to be characterized by just one sharp IR band. As reported previously,<sup>7</sup> this is near 1686.1 cm<sup>−1</sup>, a wavenumber close to those of the  $\nu(\text{Ga}–\text{H})$  modes of the gallium(II) hydrides HGaOH (1669.8 cm<sup>−1</sup>),<sup>29</sup> CH<sub>3</sub>GaH (1719.7 cm<sup>−1</sup>),<sup>22</sup> and HGaNH<sub>2</sub> (1721.8 cm<sup>−1</sup>).<sup>32</sup> With D<sub>2</sub> in place of H<sub>2</sub>, the signal exhibits the expected shift to lower wavenumber, appearing at 1206.4 (H/D = 1.3976:1), but the product derived from the reaction with HD could not be clearly identified.

**Diindium, In<sub>2</sub>.** The IR spectrum recorded after co-deposition of In vapor with an excess of argon doped with 5% H<sub>2</sub> is illustrated in Figure 5a. There were no signs of any products originating in the reactions of either In atoms or In<sub>2</sub> molecules with H<sub>2</sub>, the only detectable absorptions being attributable to traces of impurities (H<sub>2</sub>O, CO<sub>2</sub>, and CO) that could be reduced to a minimum but never wholly excluded and to addition products of these with the In atoms, viz. InCO,<sup>30</sup> In(CO)<sub>2</sub>,<sup>30</sup> and In•OH<sub>2</sub>.<sup>29</sup>

Upon photolysis of the matrix at wavelengths near 365 nm, an intense IR absorption appeared at 954.8 cm<sup>−1</sup> together with much weaker ones at 2020.8, 1079.1, 848, and 800.0 cm<sup>−1</sup> (see

**Table 2.** Wavenumbers of IR Bands Observed for Ar Matrixes Containing In<sub>2</sub> and H<sub>2</sub>/D<sub>2</sub>/HD<sup>a</sup>

H <sub>2</sub>	D <sub>2</sub>	HD	photolysis			absorber
			$\lambda = 365$ nm	$\lambda > 450$ nm	$\lambda = 365$ nm	
2020.8			↑	↓	↑	<b>1a</b>
1518	1081		↑	↑	↓	<b>3b</b>
1387.4	996.2	1387.4, 996.2				<b>InH</b>
1079.1	815.1		↑	↓	↑	<b>1b</b>
1040	1040	1040	↑	↓	↓	<b>5b</b>
954.8	693.1	899.6	↑	↓	↑	<b>1b</b>
914	914	914	↑	↓	↓	<b>5b</b>
848	630.1	611.9	↑	↓	↑	<b>1b</b>
800.0	605.4	582.3	↑	↓	↑	<b>1b</b>

<sup>a</sup> Wavenumbers are given in reciprocal centimeters.

Figure 5a). The signals built up gradually with the maximal intensities being reached only after photolysis times as long as 1.5 h. Maintaining constant relative intensities, both in buildup and decay (q.v.), the features are attributed to a common first reaction product **1b**. Clear evidence of a second distinct species **5b** came from the simultaneous growth of two other bands, one relatively strong appearing as a multiplet centered near 914 cm<sup>−1</sup> and the other very weak appearing at ca. 1040 cm<sup>−1</sup>. In addition to these features, the spectrum of the photolyzed matrix included a third family of bands absorbing at 1487.1, 713.7, and 547.6 cm<sup>−1</sup> identifiable with the HInOH molecule resulting, as reported previously,<sup>29</sup> from the photoinduced tautomerization of the adduct In•OH<sub>2</sub>. These and other spectroscopic details are listed in Table 2.

Subsequent irradiation of the matrix with broad-band visible light ( $\lambda > 450$  nm) caused a sharp decline in the intensities of the bands due to **1b**, **5b**, and HInOH (see Figure 5c). Simultaneously an absorption due to a new product **3b** appeared at 1518 cm<sup>−1</sup>. The wavenumber suggests strongly that it represents the In–H stretching mode of a terminal In(II)–H fragment [cf. the wavenumbers (in reciprocal centimeters) of other indium(II) hydrides: HInH 1548.6/1615.6,<sup>8</sup> HInOH 1486.3,<sup>29</sup> HInNH<sub>2</sub> 1530.1,<sup>32</sup> HInPH<sub>2</sub> 1546.4,<sup>33</sup> and CH<sub>3</sub>InH 1545.9<sup>22</sup>]. Visible photolysis also resulted in the appearance and growth of three other IR signals. One of these occurred at 1387.4 cm<sup>−1</sup>, a wavenumber symptomatic of the diatomic hydride InH.<sup>8</sup> The other two, occurring at 735.1 and 524.6 cm<sup>−1</sup>, could likewise be identified with InOIn<sup>34</sup> and InOH,<sup>29</sup> respectively.

Restoring the wavelength of the photolyzing radiation to ca. 365 nm led to the extinction of the absorption at 1518 cm<sup>−1</sup> and the partial recovery of intensity by the absorptions associated with **1b**. By contrast, there was no spectroscopic sign suggesting the regeneration of **5b**.

Similar experiments were also carried out with D<sub>2</sub> in place of H<sub>2</sub>. Again, there was no hint of any reaction between the primary guest species until the matrix was irradiated with light at  $\lambda =$  ca. 365 nm. The four signals at 1079.1, 954.8, 848, and 800.0 cm<sup>−1</sup> characteristic of **1b** were all observed to shift to lower wavenumber, their counterparts occurring at 815.1 (H/D = 1.3239:1), 693.1 (1.3776:1), 612 (1.3856:1), and 582.3 cm<sup>−1</sup> (1.3739:1), respectively. This behavior contrasted with the wavenumber invariance of the bands registered not only by HInOH but also by **5b**. Hence **5b**, like HInOH, must be presumed to be the product of a reaction that involves not H<sub>2</sub>

(32) Himmel, H.-J.; Downs, A. J.; Greene, T. M. *J. Am. Chem. Soc.* **2000**, *122*, 9793–9807.

(33) Himmel, H.-J.; Downs, A. J.; Greene, T. M. *Inorg. Chem.* **2001**, *40*, 396–407.

(34) Hinchcliffe, A. J.; Ogden, J. S. *J. Phys. Chem.* **1973**, *77*, 2537–2544.

(or  $D_2$ ) but some other molecule,  $H_2O$  being the obvious candidate. Switching to photolysis wavelengths in excess of 450 nm caused the decay of the bands due to both **5b** and the deuterated version of **1b** and the appearance of new bands. The most prominent of these, located at  $996.2\text{ cm}^{-1}$ , could be recognized as belonging to  $InD$  ( $H/D = 1.3927:1$ ),<sup>8</sup> but a weaker feature at  $1387.4\text{ cm}^{-1}$  confirmed that  $InH$  was also formed. The only sign of a deuterated version of **3b** was a very weak band at  $1094.6\text{ cm}^{-1}$  which appeared to correlate with the  $1518\text{ cm}^{-1}$  band of the normal version ( $H/D = 1.3868:1$ ).

In a third series of experiments  $HD$  took the place of  $H_2$  or  $D_2$ . The IR spectra of the resulting matrixes showed, after photolysis at  $\lambda = \text{ca. } 365\text{ nm}$ , three bands that could be assigned to the  $HD$  version of **1b**. These occurred at  $899.6$ ,  $630.1$ , and  $605.4\text{ cm}^{-1}$ , the first being relatively intense and the other two very weak. Of the  $HD$  version of **3b**, unfortunately, there was no obvious hint. Experiments with a roughly equimolar mixture of  $H_2$  and  $D_2$  gave rise to IR spectra that were effectively a superposition of those recorded with  $H_2$  and  $D_2$  taken separately. Hence it appeared that only one molecule of  $H_2$  (or  $D_2$ ) was involved in the primary step, which we infer to be concerted addition to  $In_2$  to form **1b**. That the product **5b** originates in the reaction of  $In_2$  with  $H_2O$  was also confirmed by carrying out an experiment in which the  $H_2O$  content of the  $H_2$ -doped matrix gas was deliberately made about 5 times greater than normal. The IR spectrum of the photolyzed matrix then showed a marked increase in the intensities of the bands due to **5b** relative to those due to **1b**, suggesting that **5b** was the dominant product of photolysis at  $\lambda = \text{ca. } 365\text{ nm}$ .

## Discussion

The main IR features observed to develop and that can be traced to the reaction of  $Ga_2$  or  $In_2$  ( $M_2$ ) with dihydrogen will be shown to arise from products of three types, viz.,  $M(\mu-H)_2M$  (**1a,b**),  $H_2MM$  ( $M = Ga$ , **2a**), and  $HMMH$  (**3a,b**). The corresponding reaction with water gives a single product,  $M(\mu-H)(\mu-OH)M$  (**5a,b**). Although the binary hydrides have been the subjects of quantum chemical studies,<sup>19,20</sup> experimental evidence of these molecules has been limited previously to  $Ga(\mu-H)_2Ga$  (identified in the earlier matrix studies of the reactions between gallium and  $H_2$ )<sup>7</sup> and  $M_2(H)OH$ , where  $M = Ga$  or  $In$  (identified somewhat speculatively in similar studies of the reactions of group 13 metal atoms with  $H_2O$ ).<sup>29</sup>

The observed IR signatures of each of the primary products **1a** and **1b** formed either thermally on deposition (in the case of **1a**) or on photolysis at  $\lambda = \text{ca. } 365\text{ nm}$  (in the case of **1b**) are suggestive of relatively symmetrical molecules in which the hydrogen atoms function exclusively as *bridging* ligands. Thus, the most intense absorptions occur at wavenumbers ( $1002$  and  $954.8\text{ cm}^{-1}$  for **1a** and **1b**, respectively) much lower than those associated with the stretching of terminal  $Ga-H$  or  $In-H$  bonds ( $>1387\text{ cm}^{-1}$ ).<sup>3,4,8,9</sup> In the case of **1a**, the wavenumber is also substantially lower than those of the IR-active  $Ga(\mu-H)_2Ga$  stretching modes of digallane,  $H_2Ga(\mu-H)_2GaH_2$  ( $1273$  and  $1202\text{ cm}^{-1}$ ).<sup>1</sup> The most plausible interpretation of the experimental results taken alone is that **1a** and **1b** are the dihydrido-bridged molecules  $Ga(\mu-H)_2Ga$  and  $In(\mu-H)_2In$ , respectively, i.e., with structure A.

The formation of **2a** by visible photolysis of **1a** and the reversal of this process under the action of near-UV or near-IR

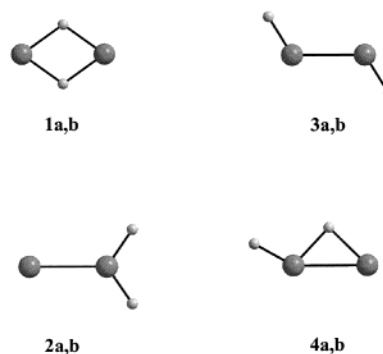


Figure 6. Geometries of the different  $M_2H_2$  isomers.

light give persuasive grounds for believing that **2a** is a second isomer of  $Ga_2H_2$ . In that case, the appearance of two bands of comparable intensity in the region associated with stretching fundamentals of terminal  $Ga-H$  bonds suggests that **2a** is  $H_2GaGa$ , i.e., structure C. The likely symmetry of the molecule and weak vibrational coupling of two  $\nu(Ga-H)$  modes not involving a common metal atom tend to rule out  $HGaGaH$  (structure B,  $C_{2h}$ ), whereas the monohydrido-bridged isomer  $Ga(\mu-H)GaH$  (structure D,  $C_s$ ) carries but a single terminal  $Ga-H$  bond.

Since **3a** and **3b** are also formed on visible photolysis of **1a** and **1b**, to which they revert with an appropriate change of photolysis conditions, it appears that they too are isomerically distinct forms of  $M_2H_2$ . There is only one high-energy IR signal to work from, but its wavenumber ( $1686.1\text{ cm}^{-1}$  for **3a** and  $1518\text{ cm}^{-1}$  for **3b**) points to the presence of at least one terminal  $M(II)-H$  bond. The most obvious molecule would then be  $HMMH$  (i.e., with the structure B), but the singly hydrido-bridged form  $HM(\mu-H)M$  (structure D) cannot be excluded on the relatively sparse spectroscopic evidence available to us.

With only two bands as reporters, the compounds **5a** and **5b** formed, it appears, from the photoinduced reaction of  $M_2$  with  $H_2O$  are less easy to identify, but the prominent features at  $951$  and  $914\text{ cm}^{-1}$  for  $M = Ga$  and  $In$ , respectively, are again strongly suggestive of  $\nu(M-H-M)$  stretching vibrations. The absence of any bands at significantly higher wavenumbers makes it unlikely that **5a** and **5b** contain terminal  $M-H$  bonds (cf.  $HMOH$ ).<sup>29</sup> Hence a possible formulation would be  $M(\mu-H)(\mu-OH)M$  with bridging hydrido and hydroxo functions, as previously suggested by Margrave et al.<sup>29</sup>

**Calculations: (i)  $M(\mu-H)_2M$ .** Detailed quantum mechanical calculations predict a minimum for the  $M_2H_2$  molecule corresponding to a singlet ground state having the planar, cyclic structure A conforming to  $D_{2h}$  symmetry (see Figure 6). The calculated dimensions, listed in Table 3, are in satisfactory agreement with the results of earlier calculations by SCF methods.<sup>19,20</sup> The  $M\cdots M$  distances are thus expected to be more than  $0.3\text{ \AA}$  longer than those in the corresponding  $M_2$  dimers each in their triplet electronic ground states, but nearly equal to that for  $M = Ga$  and shorter than that for  $M = In$  when the  $M_2$  dimers are each in their first excited singlet states. The highest occupied molecular orbital (HOMO) of  $In(\mu-H)_2In$  has  $a_g$  symmetry, whereas the lowest unoccupied molecular orbital (LUMO) formed by the p orbitals on each of the metal atoms perpendicular to the plane of the molecule has  $b_{3u}$  symmetry. The HOMO–LUMO gap is  $269.9\text{ kJ mol}^{-1}$ .

**Table 3.** Comparison between IR Spectra Observed and Calculated for  $M(\mu\text{-H})_2M$ ,  $M(\mu\text{-D})_2M$ , and  $M(\mu\text{-H})(\mu\text{-D})M$  ( $M = \text{Ga}$  or  $\text{In}$ )<sup>a</sup>

$M(\mu\text{-H})_2M$		$M(\mu\text{-D})_2M$		$M(\mu\text{-H})(\mu\text{-D})M$	
obs	calc <sup>b</sup>	obs	calc <sup>b</sup>	obs	calc <sup>b</sup>
<b>M = Ga</b>					
1220 <sup>c</sup>	1231.6 (0)	860 <sup>c</sup>	871.6 (0)	1112 <sup>c</sup>	1114.2 (47)
175 <sup>c</sup>	190.1 (0)	175 <sup>c</sup>	190.0 (0)	175 <sup>c</sup>	190.1 (0)
880	920.0 (0)	638.4	653.2 (0)	675.7	686.1 (286)
1002	1032.2 (1946)	728	735.4 (988)	953	984.2 (1181)
906.5	865.6 (213)	653.6	616.7 (108)	676 <sup>c</sup>	679.4 (114)
<i>d</i>	200.7 (18)	<i>d</i>	143.0 (9)	<i>d</i>	166.7 (14)
<b>M = In</b>					
1066.0 <sup>c</sup>	1134.2 (0)	<i>d</i>	802.5 (0)	<i>d</i>	1028.1 (55)
124.3 <sup>c</sup>	140.8 (0)	122.0 <sup>c</sup>	140.7 (0)	<i>d</i>	140.8 (0)
848	884.6 (0)	611.9	627.0 (0)	630.1	669.4 (249)
954.8	1048.5 (2268)	693.1	744.9 (1145)	899.6	983.3 (1457)
800.0	808.1 (244)	582.3	574.1 (123)	605.4	632.0 (129)
<i>d</i>	332.9 (6)	<i>d</i>	236.5 (3)	<i>d</i>	288 (5)

<sup>a</sup> Wavenumbers are given in reciprocal centimeters. <sup>b</sup> B3PW91, symmetry  $D_{2h}$ .  $\text{Ga}(\mu\text{-H})_2\text{Ga}$ :  $\text{Ga}\cdots\text{Ga}$ , 3.0425 Å;  $\text{Ga-H}$ , 1.8767 Å;  $\text{Ga-H-Ga}$ , 108.3°.  $\text{In}(\mu\text{-H})_2\text{In}$ :  $\text{In}\cdots\text{In}$ , 3.4082 Å;  $\text{In-H}$ , 2.0741 Å;  $\text{In-H-In}$ , 110.5°. Intensities (kilometers per mole) are given in parentheses. <sup>c</sup> Estimated value from a combination band harmonically corrected on the basis of a normal coordinate analysis ( $\pm 5 \text{ cm}^{-1}$ ). <sup>d</sup> Too weak to be detected or out of the range of detection in our experiments.

The triplet potential energy surface for  $M_2H_2$  also finds a minimum corresponding to a cyclic, planar structure but at an energy 106.6 ( $M = \text{Ga}$ ) or 132.5  $\text{kJ mol}^{-1}$  ( $M = \text{In}$ ) higher than that of the singlet state. Here the  $M\cdots M$  distances are shorter and the  $M\text{-H-M}$  angles are tighter.

Under  $D_{2h}$  symmetry, the six vibrational fundamentals of the  $M(\mu\text{-H})_2M$  molecule span the representations  $2a_g + b_{1u} + b_{2u} + b_{3g} + b_{3u}$  so that only three ( $b_{1u} + b_{2u} + b_{3u}$ ) are active in IR absorption. Calculations of the vibrational properties of the singlet molecules in their optimized geometries anticipate an IR spectrum dominated by a single absorption corresponding to the  $b_{1u}$  ring-stretching mode at 1020–1100  $\text{cm}^{-1}$ . This should be accompanied by a second absorption weaker by an order of magnitude corresponding to the  $b_{2u}$  ring-stretching mode at 790–900  $\text{cm}^{-1}$ . Weaker still and at risk of escaping detection in practice is the  $b_{3u}$  ring-puckering mode expected at 200–340  $\text{cm}^{-1}$ . The IR spectra of the triplet molecules are each predicted to display a similar intensity pattern but for absorptions now shifted to appreciably different wavenumbers ( $\text{Ga}_2\text{H}_2$  1147.5, 449.2, and 252.1  $\text{cm}^{-1}$ ;  $\text{In}_2\text{H}_2$  981.8, 339.7, and 275.1  $\text{cm}^{-1}$ ).

(ii) **HMMH**. The singlet potential energy surface for  $M_2H_2$  molecules includes a second minimum corresponding to structure B featuring a central  $M\text{-M}$  unit and terminal  $M\text{-H}$  bonds conforming to  $C_{2h}$  symmetry (Figure 6). The calculated dimensions are given in Table 4. The potential minimum is calculated to lie 47.5 or 74.5  $\text{kJ mol}^{-1}$  above that for  $M(\mu\text{-H})_2M$  according to whether  $M = \text{Ga}$  or  $\text{In}$ , respectively, predictions in satisfactory agreement with earlier results.<sup>19,20</sup>

Under  $C_{2h}$  symmetry the six normal modes span the representations  $3a_g + 1a_u + 2b_u$ . Once again there are three IR-active modes ( $1a_u + 2b_u$ ), but the calculations forecast high intensity for only one of these, the antisymmetric  $\nu(M\text{-H})$  vibration ( $b_u$ ) occurring at 1820–1850  $\text{cm}^{-1}$  ( $M = \text{Ga}$ ) and 1515–1540  $\text{cm}^{-1}$  ( $M = \text{In}$ ). With intensities about 2 orders of magnitude smaller than this, the other two modes are likely to occur at wavenumbers  $<200 \text{ cm}^{-1}$  and to be too weak to be seen under the present experimental conditions.

**Table 4.** Comparison between IR Spectra Observed and Calculated for HMMH, DMMH, and HMMH ( $M = \text{Ga}$  or  $\text{In}$ )<sup>a</sup>

HMMH		DMMH		HMMH	
obs	calc <sup>b</sup>	obs	calc <sup>b</sup>	obs	calc <sup>b</sup>
<b>M = Ga</b>					
<i>c</i>	1708.9 (0)	<i>c</i>	1218.3 (0)	<i>d</i>	1224.5 (255)
<i>c</i>	502.8 (0)	<i>c</i>	363.8 (0)	<i>d</i>	442.3 (5)
<i>c</i>	163.3 (0)	<i>c</i>	162.7 (0)	<i>d</i>	163.1 (0.4)
<i>d</i>	223.6 (24)	<i>d</i>	159.3 (12)	<i>d</i>	194.8 (18)
1686.1	1727.7 (1046)	1206.4	1230.9 (531)	<i>d</i>	1718.4 (534)
<i>d</i>	186.2 (53)	<i>d</i>	132.7 (27)	<i>d</i>	151.9 (34)
<b>M = In</b>					
<i>c</i>	1505.5 (0)	<i>c</i>	1070.0 (0)	<i>d</i>	1074.1 (300)
<i>c</i>	406.2 (0)	<i>c</i>	291.3 (0)	<i>d</i>	356.4 (4)
<i>c</i>	93.1 (0)	<i>c</i>	92.8 (0)	<i>d</i>	92.9 (0.02)
<i>d</i>	168.0 (18)	<i>d</i>	119.3 (9)	<i>d</i>	145.8 (14)
1518	1517.9 (1230)	1081	1078.4 (621)	<i>d</i>	1511.8 (625)
<i>d</i>	152.2 (36)	<i>d</i>	108.1 (18)	<i>d</i>	123.9 (23)

<sup>a</sup> Wavenumbers are given in reciprocal centimeters.

**Table 5.** Comparison between IR Spectra Observed and Calculated for  $\text{GaGaH}_2$ ,  $\text{GaGaD}_2$ , and  $\text{GaGaHD}$  and IR Spectra Calculated for  $\text{InInH}_2$ ,  $\text{InInD}_2$ , and  $\text{InInHD}$ <sup>a</sup>

MMH <sub>2</sub>		MMD <sub>2</sub>		MMHD	
obs	calc <sup>b</sup>	obs	calc <sup>b</sup>	obs	calc <sup>b</sup>
<b>M = Ga</b>					
1752.1	1835.8 (509)	1260.1	1304.3 (258)	1269.6	1312.1 (215)
752	770.0 (367)	540.3	549.7 (179)	655.4	672.0 (276)
<i>c</i>	179.3 (13)	<i>c</i>	178.1 (13)	<i>c</i>	177.3 (14)
<i>c</i>	359.2 (73)	<i>c</i>	260.6 (37)	<i>c</i>	314.6 (55)
1765.1	1847.7 (370)	1275.8	1318.9 (190)	1758	1841.4 (447)
<i>c</i>	224.4 (23)	<i>c</i>	161.4 (11)	<i>c</i>	185.7 (14)
<b>M = In</b>					
	1601.7 (607)		1136.0 (307)		1600.5 (492)
	652.3 (510)		464.0 (253)		568.3 (385)
	118.9 (6)		118.5 (6)		118.6 (6)
	304.5 (74)		218.8 (37)		265.1 (55)
	1599.9 (355)		1137.9 (180)		1137.5 (232)
	179.0 (17)		128.4 (8)		146.8 (11)

<sup>a</sup> Wavenumbers are given in reciprocal centimeters. <sup>b</sup> B3PW91, symmetry  $C_{2v}$ .  $\text{GaGaH}_2$ :  $\text{Ga-Ga}$ , 2.7091 Å;  $\text{Ga-H}$ , 1.6001 Å;  $\text{H-Ga-H}$ , 109.9°.  $\text{InInH}_2$ :  $\text{In-In}$ , 3.1211 Å;  $\text{In-H}$ , 1.7767 Å;  $\text{H-In-H}$ , 109.5°. Intensities (kilometers per mole) are given in parentheses. <sup>c</sup> Too weak to be detected or out of the range of detection in our experiments.

(iii) **MMH<sub>2</sub>**. As noted previously,<sup>19,20</sup> there is a third minimum in the singlet potential energy surface. This corresponds to a mixed-valence isomer in which the two H atoms are bound not to different M atoms, as in structure B, but to the *same* M atom of an  $M\text{-M}$  unit, as in structure C. The optimum geometry is then planar so that the molecule assumes  $C_{2v}$  symmetry (Figure 6 and Table 5). Calculations past and present are agreed that this isomer is somewhat more stable than the *trans*- $C_{2h}$  one (by 49.7 and 30.0  $\text{kJ mol}^{-1}$  for  $M = \text{Ga}$  and  $\text{In}$ , respectively, according to our MP2 estimates).

The six vibrational fundamentals of  $\text{MMH}_2$  ( $3a_1 + 1b_1 + 2b_2$ ) are all IR-active. However, three of them are expected to give absorptions appreciably more intense than the rest. Two of these correspond to the  $\nu(M\text{-H})$  modes with predicted wavenumbers at 1810–1850  $\text{cm}^{-1}$  ( $M = \text{Ga}$ ) and 1600–1645  $\text{cm}^{-1}$  ( $M = \text{In}$ ), i.e., 80–100  $\text{cm}^{-1}$  higher than for the analogous modes of the HMMH isomers. The third, associated with the  $\text{MH}_2$  scissoring motion, is likely to occur in the neighborhood of 750–775 and 650–695  $\text{cm}^{-1}$  for  $M = \text{Ga}$  and  $\text{In}$ , respectively.

(iv) **HM( $\mu\text{-H}$ )M**. Intermediate in stability between HMMH and  $\text{MMH}_2$  is a fourth isomer with the monohydrido-bridged



**Table 6.** Calculated Dimensions, Wavenumbers, and IR Intensities for  $\text{HM}(\mu\text{-H})\text{M}$  ( $\text{M} = \text{Ga}$  or  $\text{In}$ )

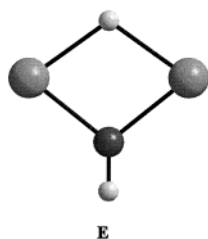
property	$\text{HGa}(\mu\text{-H})\text{Ga}$	$\text{HIn}(\mu\text{-H})\text{In}$
symmetry	$C_s$	$C_s$
	Dimensions <sup>a</sup>	
$\text{M}(1)\text{--M}(2)$	2.6258	3.0674
$\text{M}(1)\text{--H}_b$	1.8729	2.1150
$\text{M}(2)\text{--H}_b$	1.9290	2.0692
$\text{M}(1)\text{--H}_t$	1.6137	1.7987
$\text{M}(1)\text{--H}_b\text{--M}(2)$	87.4	94.3
$\text{H}_t\text{--M}(1)\text{--H}_b$	102.9	101.4
	Vibrations <sup>b</sup>	
$\nu_1$ ( $a'$ )	1753.3 (731)	1536.7 (831)
$\nu_2$ ( $a'$ )	1164.7 (347)	1018.8 (406)
$\nu_3$ ( $a'$ )	822.3 (436)	775.1 (585)
$\nu_4$ ( $a'$ )	400.8 (11)	366.2 (5)
$\nu_5$ ( $a'$ )	168.6 (9)	102.3 (5)
$\nu_6$ ( $a''$ )	197.3 (13)	203.5 (12)

<sup>a</sup> DFT (B3PW91) calculations. Distances are given in angstroms; bond angles are given in degrees.  $b$  = bridging,  $t$  = terminal. <sup>b</sup> Wavenumbers are given in reciprocal centimeters. IR intensities (in parentheses) are given in kilometers per mole.

structure D, and also having a singlet ground state. Figure 6 illustrates the optimized geometry deduced on the basis of our quantum chemical calculations. Bond distances given in Table 6 (in angstroms) compare well with the previous SCF estimates.<sup>19,20</sup> According to our MP2 calculations, the local PE minimum defining the monobridged isomer  $\text{HM}(\mu\text{-H})\text{M}$  lies 33.5 and 55.2 kJ mol<sup>−1</sup> above the minimum defining the dibridged isomer  $\text{M}(\mu\text{-H})_2\text{M}$  for  $\text{M} = \text{Ga}$  and  $\text{In}$ , respectively.

The IR spectra simulated for the  $\text{HM}(\mu\text{-H})\text{M}$  isomers comprise all six fundamental transitions ( $5a' + 1a''$ ), of which only three appear with substantial intensity. Stretching of the unique terminal  $\text{M}\text{--H}$  bond accounts for one of these with a calculated wavenumber of 1730–1805 and 1530–1560 cm<sup>−1</sup> (cf.  $\text{HMMH}$ ). Stretching of the  $\text{M}\text{--H}\text{--M}$  bridge accounts for the other two; in this case the calculated wavenumbers are 1140–1165 and 805–825 cm<sup>−1</sup> for  $\text{M} = \text{Ga}$  and 1015–1070 and 750–775 cm<sup>−1</sup> for  $\text{M} = \text{In}$  [cf.  $\text{M}(\mu\text{-H})_2\text{M}$ ].

(v)  $\text{M}_2(\text{H})\text{OH}$ . According to our quantum chemical calculations, the most stable form of this molecule is singlet  $\text{M}(\mu\text{-H})(\mu\text{-OH})\text{M}$  (structure E) with bridging H and OH ligands forming a planar, cyclic array with  $C_{2v}$  symmetry.  $\text{M}\text{--H}$  distances are calculated to be 1.8908 and 2.0696 Å and  $\text{M}\text{--O}$  distances to be 2.0070 and 2.1352 Å for  $\text{M} = \text{Ga}$  and  $\text{In}$ , respectively. The IR spectra predicted for the molecules are each dominated by a single absorption at 990.0 and 996.7 cm<sup>−1</sup> corresponding to the  $b_2$   $\text{Ga}\text{--H}\text{--Ga}$  and  $\text{In}\text{--H}\text{--In}$  stretching motion, respectively, and with an intensity nearly 20 times that of any other mode. This feature should therefore be located some 40–50 cm<sup>−1</sup> to low wavenumber of its  $b_{1u}$  counterpart in the spectrum of  $\text{M}(\mu\text{-H})_2\text{M}$ .



**Assignment of the Matrix Products:  $\text{M}(\mu\text{-H})_2\text{M}$  [ $\text{M} = \text{Ga}$  (1a) or  $\text{In}$  (1b)].** Figure 7 compares the IR spectra of each of

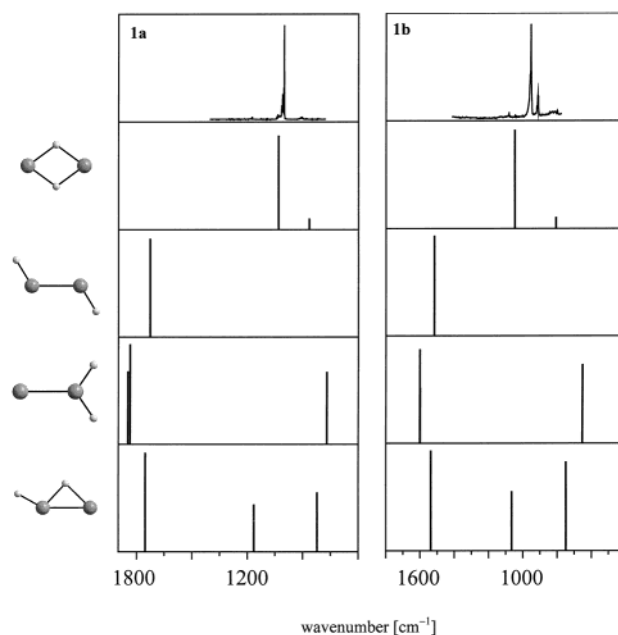


**Figure 7.** (a) Comparison between the observed IR absorptions of species **1a** and those calculated for  $\text{Ga}(\mu\text{-H})_2\text{Ga}$ ,  $\text{HGaGaH}$ ,  $\text{GaGaH}_2$ , and  $\text{HGa}(\mu\text{-H})\text{Ga}$ . (b) Comparison between the observed IR absorptions of species **1b** and those calculated for  $\text{In}(\mu\text{-H})_2\text{In}$ ,  $\text{HInInH}$ ,  $\text{InInH}_2$ , and  $\text{HIn}(\mu\text{-H})\text{In}$ .

the primary products **1a** and **1b** with those modeled for the molecules  $\text{M}(\mu\text{-H})_2\text{M}$ ,  $\text{HMMH}$ ,  $\text{MMH}_2$ , and  $\text{HM}(\mu\text{-H})\text{M}$ , where  $\text{M} = \text{Ga}$  and  $\text{In}$ , respectively. Hence it is evident that the experimental results are consistent with only one of these isomers, namely,  $\text{M}(\mu\text{-H})_2\text{M}$ . The intense IR absorption at 1002 cm<sup>−1</sup> and the much weaker one at 906.5 cm<sup>−1</sup> then represent the  $b_{1u}$  and  $b_{2u}$  ring-stretching modes, respectively, of the  $\text{Ga}(\mu\text{-H})_2\text{Ga}$  molecule, with the corresponding features of  $\text{In}(\mu\text{-H})_2\text{In}$  occurring at 954.8 and 800.0 cm<sup>−1</sup>. How closely the molecules parallel each other in their observed spectroscopic properties is underlined by the finding that each displays three other weak bands that remain to be accounted for; these occur at 2200, 1176, and 880 cm<sup>−1</sup> in the spectrum of the gallium compound and at 2020.8, 1079.1, and 848 cm<sup>−1</sup> in the spectrum of its indium analogue.

The only realistic interpretation of the two high-frequency transitions in each spectrum is that they represent combination modes, that at 2200 or 2020.8 cm<sup>−1</sup> arising from  $\nu_1$  ( $a_g$ ) +  $\nu_3$  ( $b_{1u}$ ) and that at 1176 or 1079.1 cm<sup>−1</sup> from  $\nu_2$  ( $a_g$ ) +  $\nu_3$  ( $b_{1u}$ ). In close proximity to the  $b_{1u}$  fundamental, the latter undoubtedly gains enhanced intensity through Fermi resonance. If these assignments are correct, it follows that  $\nu_1$  ( $a_g$ ) = 1220 cm<sup>−1</sup> and  $\nu_2$  ( $a_g$ ) = 174 cm<sup>−1</sup> for  $\text{Ga}(\mu\text{-H})_2\text{Ga}$  and that  $\nu_1$  ( $a_g$ ) = 1066.0 cm<sup>−1</sup> and  $\nu_2$  ( $a_g$ ) = 124.3 cm<sup>−1</sup> for  $\text{In}(\mu\text{-H})_2\text{In}$ .

No such interpretation offers itself for the remaining feature at 880 cm<sup>−1</sup> [ $\text{Ga}(\mu\text{-H})_2\text{Ga}$ ] or 848 cm<sup>−1</sup> [ $\text{In}(\mu\text{-H})_2\text{In}$ ]. Instead we propose that this arises from the  $b_{3g}$  ring-stretching mode made active in IR absorption in the unsymmetrical isotopomers  $^{69}\text{Ga}(\mu\text{-H})_2^{71}\text{Ga}$  (48%) and  $^{113}\text{In}(\mu\text{-H})_2^{115}\text{In}$  (8.2%) and intensified through coupling with the  $b_{2u}$  fundamental, which now assumes the same irreducible representation ( $b_2$ ). To substantiate this idea, we have performed a calculation based on a harmonic potential, fitting the potential constants empirically to the wavenumbers observed (a) for  $\nu_1$ ,  $\nu_2$ ,  $\nu_4$ , and  $\nu_5$  of the symmetrical species  $^{69}\text{Ga}_2\text{H}_2$  and  $^{69}\text{Ga}_2\text{D}_2$  and (b) for  $\nu_1$  (952

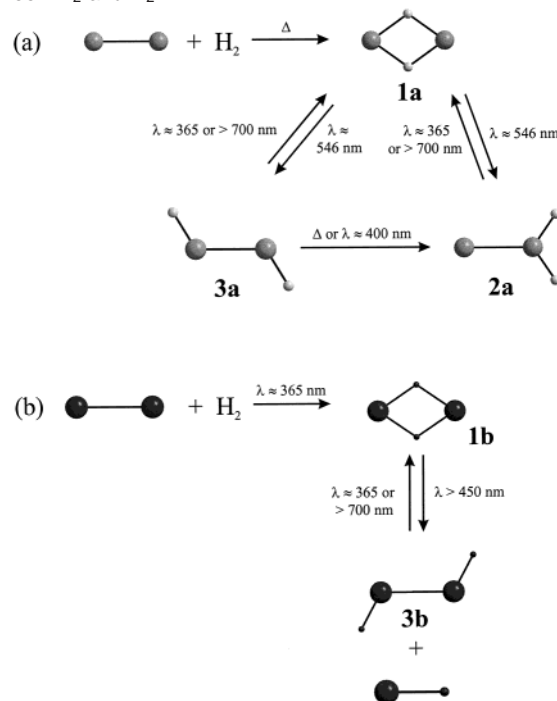
$\text{cm}^{-1}$ ),  $\nu_4$  ( $676\text{ cm}^{-1}$ ), and  $\nu_5$  ( $1112\text{ cm}^{-1}$ ) of  $^{69}\text{Ga}_2\text{HD}$ . With these constraints, the  $\text{b}_{3g}$  ring-stretching mode of  $^{69}\text{Ga}_2\text{H}_2$  is then predicted to occur near  $887\text{ cm}^{-1}$ , i.e., encouragingly close to the weak absorption observed near  $880\text{ cm}^{-1}$ . We then used the model to predict isotope shifts and eigenvectors for the other  $^{69}\text{Ga}^{71}\text{Ga}$ - and  $^{71}\text{Ga}_2$ -containing isotopic species. Hence it emerged, first, that the  $^{69}\text{Ga}_2/^{71}\text{Ga}_2$  shift of  $\nu_2$  is in good agreement with the observed value ( $2.5$  vs  $2.7\text{ cm}^{-1}$ ) and, second, that the predicted H/D shift is very small (less than  $0.2\text{ cm}^{-1}$ ). On this basis we can assign the weak features near  $1128\text{ cm}^{-1}$  for  $\text{Ga}_2\text{HD}$  and  $906\text{ cm}^{-1}$  for  $\text{Ga}_2\text{D}_2$  to the respective  $\nu_2 + \nu_4$  combinations, while the weak band near  $849\text{ cm}^{-1}$  for  $\text{Ga}_2\text{HD}$  would be appropriate for the  $\nu_2 + \nu_5$  one. Next we can make use of the calculated eigenvectors for the  $^{69}\text{Ga}^{71}\text{GaH}_2$  isotopomer to predict (assuming the harmonic approximation in both mechanical and electrical terms) the ratio of the IR intensities,  $I(\nu_3)/I(\nu_4)$ , for this molecule possessing as it does not  $D_{2h}$  but  $C_{2v}$  symmetry. With due allowance for the statistical abundance of the isotopomer (48%), this leads us to expect an intensity for  $\nu_3$  about 1% that for  $\nu_4$  (which gives rise to the most intense band in the spectrum). The experimental finding that the band at  $880\text{ cm}^{-1}$  has an intensity  $1.5\% \pm 0.5\%$  that of the band at  $1002\text{ cm}^{-1}$  bears out our interpretation, in the case of  $\text{Ga}_2\text{H}_2$  at least.

For  $\text{Ga}(\mu\text{-H})_2\text{Ga}$  and  $\text{In}(\mu\text{-H})_2\text{In}$ , therefore, all but one of the six vibrational fundamentals have been located, albeit with varying degrees of assurance, on the basis of the observed spectra. The results are in every case consistent not only with the effects of deuteration, whether partial in  $\text{M}(\mu\text{-H})(\mu\text{-D})\text{M}$  or complete in  $\text{M}(\mu\text{-D})_2\text{M}$ , where these can be observed, but also with the vibrational properties forecast by the quantum chemical calculations.

**$\text{H}_2\text{MM}$  [ $\text{M} = \text{Ga}$  (**2a**)].** Product **2a** is characterized by strong absorptions at  $1765.1$ ,  $1752.1$ , and  $752\text{ cm}^{-1}$ , enabling it to be identified as the isomer  $\text{H}_2\text{GaGa}$ . As revealed in Table 5, DFT calculations anticipate well the wavenumbers, intensity pattern, and isotopic shifts displayed by the molecule. The experiments failed, however, to give any sign of the corresponding indium species,  $\text{H}_2\text{InIn}$ .

**HMMH [ $\text{M} = \text{Ga}$  (**3a**) or  $\text{In}$  (**3b**)].** Somewhat more problematic is the identification of the products **3a** and **3b** formed on visible photolysis of **1a** and **1b**, respectively. Unfortunately neither is characterized by more than a single, relatively weak absorption in the high-wavenumber region of the IR spectrum. The wavenumbers of  $1686.1$  (**3a**) and  $1518\text{ cm}^{-1}$  (**3b**) point to the stretching vibration of a terminal  $\text{M}(\text{II})\text{-H}$  unit. The two most likely options are HMMH and  $\text{HM}(\mu\text{-H})\text{M}$ ; the  $\nu(\text{M-H})$  modes of  $\text{MMH}_2$  are expected to occur at wavenumbers significantly higher than those observed for **3a** and **3b** (see Tables 4 and 5), and the spectra should display a second feature of comparable intensity at lower wavenumber. In the circumstances, the observation of a single IR band appears to be more consistent with HMMH than with  $\text{HM}(\mu\text{-H})\text{M}$ , for which transitions of appreciable intensity would be anticipated in the region associated with  $\nu(\text{M-H-M})$  vibrations ( $800\text{--}1100\text{ cm}^{-1}$ ). This contrasts with the *trans*- $C_{2h}$  HMMH molecule, which is expected to be characterized by a single strong IR absorption at high wavenumber due to the  $\text{b}_u$   $\nu(\text{M-H})$  fundamental and no other at wavenumbers  $> 200$

**Scheme 1.** Thermally and Photolytically Activated Reactions Taking Place in Ar Matrixes (a) between  $\text{Ga}_2$  and  $\text{H}_2$  and (b) between  $\text{In}_2$  and  $\text{H}_2$



<sup>b</sup> B3PW91, symmetry  $C_{2h}$ . HGaGaH: Ga–Ga, 2.5848 Å; Ga–H, 1.6261 Å; Ga–Ga–H,  $121.3^\circ$ . HInInH: In–In, 3.0596 Å; In–H, 1.8136 Å; In–In–H,  $120.2^\circ$ . Intensities (kilometers per mole) are given in parentheses. <sup>c</sup> Inactive in IR absorption. <sup>d</sup> Too weak to be detected or out of the range of detection in our experiments.

$\text{cm}^{-1}$ , in keeping with the apparent simplicity of the spectra due to **3a** and **3b**.

**$\text{M}(\mu\text{-H})(\mu\text{-OH})\text{M}$  [ $\text{M} = \text{Ga}$  (**5a**) or  $\text{In}$  (**5b**)].** The products **5a** and **5b** are most plausibly assigned the structures  $\text{M}(\mu\text{-H})(\mu\text{-OH})\text{M}$  on the basis of the circumstances of the experiments and of their observed IR signatures. Moreover, the DFT calculations find no  $\text{M}_2(\text{H})\text{OH}$  isomer better able than this to account for the experimental spectra. The prominent IR absorptions at  $951$  and  $914.0\text{ cm}^{-1}$  are then the obvious candidates for the antisymmetric  $\nu(\text{Ga-H-Ga})$  and  $\nu(\text{In-H-In})$  mode,  $\nu_7$  ( $\text{b}_2$ ), respectively.

**Reaction Pathways.** Scheme 1 formulates a reaction scheme for the formation, isomerization, and decomposition of the singlet  $\text{M}(\mu\text{-H})_2\text{M}$  molecules. Although there is much common ground between  $\text{Ga}_2$  and  $\text{In}_2$  in their reactions with both  $\text{H}_2$  and  $\text{H}_2\text{O}$ , one notable difference is to be found in the activation of the reactions:  $\text{Ga}_2$  reacts spontaneously, even at low temperatures, whereas  $\text{In}_2$  requires relatively high energy photoexcitation ( $\lambda = \text{ca. } 365\text{ nm}$ ).

The general consensus appears now to be that  $\text{Ga}_2$  and  $\text{In}_2$  each have triplet ground states [ $X^3\Pi(0_u^-)$ ]. This is also the case on the evidence of our quantum chemical calculations, which impute such a state to both molecules with bond distances (in the order MP2/B3PW91/B3LYP) of  $2.7370/2.7147/2.7491\text{ Å}$  and  $3.1342/3.1485/3.1746\text{ Å}$  for  $\text{Ga}_2$  and  $\text{In}_2$ , respectively, in good agreement with the results of earlier calculations.<sup>28,35</sup> At  $169.1/162.3/155.1$  and  $106.0/103.5/98.2\text{ cm}^{-1}$ , the corresponding vibrational wavenumbers also tally satisfactorily with the

(35) Balasubramanian, K. *J. Phys. Chem.* **1986**, *90*, 6786–6790.

experimental values of 180 and 118  $\text{cm}^{-1}$  reported by Froben et al.<sup>28</sup> By contrast, the singlet state ( $^1\Sigma_g^+$ ) is characterized by a longer bond (3.0463/3.0251/3.0642 and 3.5117/3.4799/3.5082 Å, respectively) and rather lower vibrational wavenumber (137.2/135.7/131.1 and 86.7/90.8/87.2  $\text{cm}^{-1}$ ). Of particular interest is the triplet–singlet energy gap, which we estimate to be 62.6 and 50.6  $\text{kJ mol}^{-1}$  for  $\text{Ga}_2$  and  $\text{In}_2$ , respectively. Earlier calculations suggest a value of 56.7  $\text{kJ mol}^{-1}$  for  $\text{Ga}_2$ .<sup>35</sup> It has even been suggested<sup>27</sup> on the evidence of the electronic absorption spectra that singlet  $\text{Al}_2$  and  $\text{Ga}_2$  molecules are present in the matrixes formed by trapping the metal vapors with an excess of a noble gas, triplet–singlet excitation being achieved possibly by the light emitted by the furnace.

As indicated in the previous section, the  $\text{M}(\mu\text{-H})_2\text{M}$  molecules each have a singlet ground state, the triplet state lying 117.6 and 129.0  $\text{kJ mol}^{-1}$  to higher energy. Hence we calculate that the reaction of the triplet  $\text{M}_2$  molecule with  $\text{H}_2$  to form triplet  $\text{M}(\mu\text{-H})_2\text{M}$  is weakly endothermic with energies of +19.4 and +17.6  $\text{kJ mol}^{-1}$ , whereas the reaction energy for the formation of singlet  $\text{M}(\mu\text{-H})_2\text{M}$  is −98.2 and −109.4  $\text{kJ mol}^{-1}$  for  $\text{M} = \text{Ga}$  and  $\text{In}$ , respectively. By contrast, the corresponding reactions of singlet  $\text{M}_2$  are all exothermic, the energies being −17.4 and −30.1  $\text{kJ mol}^{-1}$  for the formation of triplet  $\text{M}(\mu\text{-H})_2\text{M}$  and −135.0 and −157.1  $\text{kJ mol}^{-1}$  for the formation of the singlet molecule. A tenable scheme for the reaction of ground-state  $\text{M}_2$  with  $\text{H}_2$  would entail the initial formation of  $\text{M}(\mu\text{-H})_2\text{M}$  in its excited triplet state, followed by quenching to the singlet ground state with the help of the matrix cage. According to our DFT calculations, however, the initial step would not be expected to proceed spontaneously.

This accords with the matrix behavior of  $\text{In}_2 + \text{H}_2$  but not of  $\text{Ga}_2 + \text{H}_2$ , which does appear to react spontaneously, even at matrix temperatures. The kinetic isotope effect observed for the  $\text{Ga}_2 + \text{D}_2$  reaction implies, however, that the second reaction does present a small activation barrier, which is readily overcome by the parent molecule  $\text{H}_2$  and even  $\text{HD}$  but not by the totally deuterated one. Rough estimations based on differences in zero-point energies would bracket a value between 35 and 44  $\text{kJ mol}^{-1}$ . It may be noted that the IR radiation energy necessary to activate the  $\text{Ga}_2 + \text{D}_2$  reaction (4500–3200  $\text{cm}^{-1}$ )

corresponds to values between 53 and 38  $\text{kJ mol}^{-1}$ , in relatively good agreement with the estimated triplet–singlet energy gap of 56.7  $\text{kJ mol}^{-1}$  for  $\text{Ga}_2$ .<sup>35</sup> This effect seems to rule out the possibility that a fraction of the  $\text{Ga}_2$  molecules present in the matrix is in the  $^1\Sigma_g^+$  state and so has access to a strongly exothermic reaction channel leading more or less directly to singlet  $\text{Ga}(\mu\text{-H})_2\text{Ga}$ . That  $\text{In}_2$  does not follow suit, requiring photoactivation for its reaction with  $\text{H}_2$ , would then be attributable to an increase in the energy barrier that parallels the increase in the triplet–singlet gap in  $\text{In}_2$  compared with  $\text{Ga}_2$ .

Any attempt to explain the difference in reactivity between  $\text{Ga}_2$  and  $\text{In}_2$  needs also to take account of other low-lying triplet states. In the  $^3\Pi_u$  ground state the unpaired electrons occupy different orbitals to give the configuration  $\sigma_g^2\sigma_u^2\pi_g^1\pi_u^1$ . Very close in energy is a second triplet state,  $^3\Sigma_g^-$ , corresponding to the configuration  $\sigma_g^2\sigma_u^2\pi_u^2$ . For  $\text{Ga}_2$  the  $^3\Sigma_g^- - ^3\Pi_u$  energy gap is estimated to be minuscule (ca. 2  $\text{kJ mol}^{-1}$ ), but for  $\text{In}_2$  it is rather larger (10.5  $\text{kJ mol}^{-1}$ ). The  $^3\Sigma_g^-$  state with its increased electron density in the frontier  $\pi_u$  orbitals may well be better adapted than the  $^3\Pi_u$  one to attractive interaction with the  $\text{H}_2$  molecule, thereby reducing the barrier opposing addition. In that case, too, differences of energy and/or lifetime could be important in dictating the conditions of reaction. Without a fuller knowledge of the  $\text{Ga}_2$  and  $\text{In}_2$  dimers, however, it is impossible to come to any more definite conclusions about their relative reactivities.

**Acknowledgment.** We thank (i) the Deutsche Forschungsgemeinschaft for financial support and the award of a Habilitation grant to H.-J.H., (ii) CNRS for support of the research at Paris (L.M.), and (iii) the EPSRC for support of the research at Oxford (A.J.D.).

**Supporting Information Available:** Three figures showing IR difference spectra, orbitals of  $\text{In}(\mu\text{-H})_2\text{In}$ , and geometries of  $\text{M}_2\text{H}(\text{OH})$  species, and two tables showing properties of  $\text{M}(\mu\text{-H})(\mu\text{-OH})\text{M}$ ,  $\text{HM}(\mu\text{-OH})\text{M}$ , and  $\text{HMMOH}$  from DFT calculations (PDF). This information is available free of charge via the Internet at <http://pubs.acs.org>.

JA0122795